ACS OMEGA

http://pubs.acs.org/journal/acsodf

Article

Radical Photopolymerization Using 1,4-Dihydropyrrolo[3,2-*b*]pyrrole Derivatives Prepared via One-Pot Synthesis

Yuanyuan Xu, Yu Chen,* Xuguang Liu, and Song Xue

Cite This: *ACS Omega* 2021, 6, 20902−20911

Read Online

ACCESS | Metrics & More | Article Recommendations | Supporting Information

ABSTRACT: Radical photopolymerization has attracted significant attention for manufacturing products with complicated structures. Herein, the synthesized 1,4-bis(4-bromophenyl)-2,5-bis(4-nitrophenyl)-1,4-dihydropyrrole[3,2-b]pyrrole (PyBN) is found to show varying photoactivity upon irradiation at different wavelengths. PyBN affords two main absorption bands, and its maximum absorption peak is at 462 nm, attributing to its strong intramolecular charge transfer property based on the donor−acceptor structure. It efficiently photoinitiates the radical photopolymerization of different (meth)acrylate materials under 365 and 395 nm LED irradiation. The highest double bond conversion of 99.86% is achieved for these materials. Under 470 nm LED, PyBN does not show molecular structure change from photolysis results as a result of intramolecular charge transfer. Therefore, PyBN shows wavelength-selective photoactivity with potential application in dual-wavelength volumetric additive manufacturing. A unique solid product is successfully fabricated using a 365 nm LED with co-irradiation of a 470 nm LED. Additionally, PyBN incorporating camphorquinone (CQ) as a two-component visible light photoinitiator system is investigated under 470 nm LED irradiation. As PyBN has a charge transfer activity at 470 nm, the combination with CQ exhibits a good synergistic interaction. Besides nitro-based PyBN, a methyl-based PyBC was prepared as a reference compound.

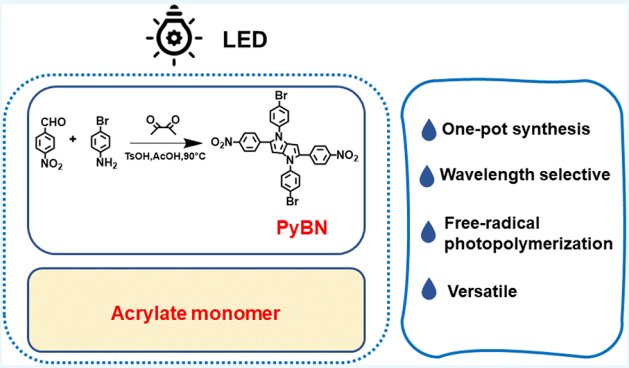

1. INTRODUCTION

Photopolymerization is a popular technique for curing materials used in applications such as three-dimensional (3D) printing, adhesives, and coatings.[1−6] Photoinitiated photopolymerization affords advantages such as low temperature, no usage of harmful solvents, a rapid curing rate, and spatial control of polymerization compared to the features of thermal curing. Radical photopolymerization has attracted increasing attention to obtain products with 3D structures by different additive manufacturing techniques[7−12] such as layer-wise and volumetric methods.[13,14] The curing principle of radical photosensitive resins is similar.[15,16] Generally, the photosensitive resin used for radical photopolymerization is composed of monomers and a prepolymer containing C═C double bonds as well as a photoinitiator and co-initiator that matches a specific light wavelength.[17,18] (Meth)acrylate resin is a commonly used photoactive material both in academic and practical applications that yields a good cross-linked polymer via radical polymerization.[19−25]

A photoinitiator is important to drive the photopolymerization reaction after light irradiation. The design of new photoinitiators for radical photopolymerization has shown significant advancement in preventing oxygen inhibition, affording rapid photopolymerization, and expanding the spectral range to visible and near-infrared (NIR) regions.[26−28] Photoactive (keto) coumarins and camphorquinone (CQ) are commonly employed as radical photoinitiators for 3D printing.[29,30] According to the literature reports, volumetric 3D printing involves a unique dual-wavelength polymerization and continuously confines the photopolymerized region through a multi-component system composed of photoinitiators, photoinhibitors, and photopolymerizable resins.[13,31] Among these components, the photoinitiators are formulated using CQ and ethyl 4-(dimethylamino)benzoate (EDAB) as the visible light photoinitiator and co-initiator, respectively. In this work, tetraaryl-1,4-dihydropyrrolo[3,2-*b*]pyrrole synthesized in our laboratory was found to show significant potential in radical photopolymerization systems as well as in combination with CQ as a substitute for the CQ/EDAB

Received: May 4, 2021
Accepted: July 23, 2021
Published: August 5, 2021

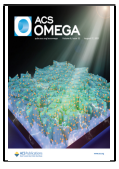

ACS Publications

© 2021 The Authors. Published by American Chemical Society

https://doi.org/10.1021/acsomega.1c02338
ACS Omega 2021, 6, 20902−20911

Scheme 1. Synthetic Route of PyBN and Its Multiple Applications

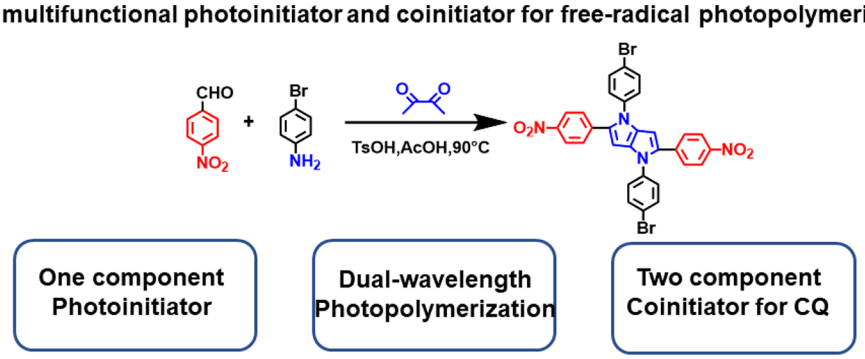

photoinitiator system. To our knowledge, 1,4-dihydropyrrolo-[3,2-*b*]pyrrole and its derivatives have not been investigated for photopolymerization to date.

Since their development in 1972, 1,4-dihydropyrrolo[3,2-*b*]pyrroles have been used in various fields including resistive memory devices, organic solid-state emitters, and organic light-emitting diodes.[32−36] These are promising alternatives to furans and thiophenes and can be prepared via a simple one-pot synthesis with easy purification and moderate yields. The reported 1,4-dihydropyrrolo[3,2-*b*]pyrroles have wide absorption bands, which can be easily tuned by structural modifications.[37,38] The pyrrolo[3,2-*b*]pyrrole compound synthesized in our laboratory is found to induce radical photopolymerization of various (meth)acrylate monomers and prepolymers. Its role in photopolymerization is affected by different wavelengths of light, and this type of material has a great potential in being used in dual-wavelength photopolymerization. The investigations of the properties of pyrrolo[3,2-*b*]pyrrole-based systems should be further investigated.

Herein, the synthesis of 1,4-bis(4-bromophenyl)-2,5-bis(4-nitrophenyl)-1,4-dihydropyrrole[3,2-*b*]pyrrole (PyBN) is reported for its application to radical photopolymerization under different irradiation wavelengths. Scheme 1 shows the synthetic route of PyBN. Using one-pot synthesis, the target product is successfully obtained in moderate yields via the reaction of aromatic aldehydes with *p*-anisidine and butane-2,3-dione in acetic acid at 90 °C. As shown in Scheme 1, PyBN is a multifunctional photoinitiator and co-initiator for radical photopolymerization and also can be used for dual-wavelength photopolymerization. The absorption properties, emission spectra, and steady-state photolysis are studied under light-emitting diode (LED) irradiation at 365, 395, and 470 nm. The capability of PyBN to induce radical photopolymerization of (meth)acrylate formulations is evaluated. The C═C double bond conversion in PyBN-based photopolymerization systems employing different monomers and prepolymers is compared. Wavelength selectivity of PyBN is studied, and a possible application of volumetric photopolymerization using a dual-wavelength light source is demonstrated. In addition, PyBN is successfully used as an alternative to EDAB to incorporate CQ, and CQ/PyBN can be used as a two-component visible-light photoinitiator system. CQ/PyBN induces TMPTA polymerization with an efficiency similar to CQ/EDAB under LED irradiation at 470 nm, indicating a synergistic effect between CQ and PyBN. Therefore, pyrrole[3,2-*b*]pyrrole-based compounds show significant potential for application in different radical photopolymerization systems that can exhibit good curing performances. This work can provide an experimental basis and guide the design of new photopolymerization systems in the future.

2. EXPERIMENTAL SECTION

2.1. Materials. 4-Nitrobenzaldehyde, 4-bromoaniline, 2,3-butanedione, *p*-toluene sulfonic acid, and anhydrous acetic acid were purchased from Energy Chemical. The used acrylate resin includes trimethylolpropane triacrylate (TMPTA), triethylene glycol dimethacrylate (TEGDMA), hexamethylene diacrylate (HDDA), dipropylene glycol acrylate (DPGDA), tri(propylene glycol) diacrylate (TPGDA), and polyethylene glycol acrylate (PEGDA), which were purchased from Tokyo Chemical Industry. A polyester acrylate resin (PEO 2257) and a polyurethane acrylate (PUA 5268) were obtained from Shanghai Baorun Chemical Co. Ltd. Bisphenol A-glycidyl methacrylate (Bis-GMA) was purchased from Sigma-Aldrich. Materials were all available commercially and did not require further purification. The main materials used in this work have been exhibited in Figure 2b (Section 3.1).

2.2. Instruments. The nuclear magnetic resonance (NMR) spectra were recorded in deuterated chloroform ($CDCl_3$) or dimethylsulfoxide (DMSO-d_6) with a Bruker AM-400 spectrometer (400 MHz for ^{1}H NMR and 100 MHz for ^{13}C NMR). The reported chemical shifts were against TMS. Ultraviolet−visible measurements were performed on a SHIMADZU UV-2600 spectrophotometer. For the fluorescence spectra, a HITACHI F-4500 fluorescence spectrophotometer was used. Cyclic voltammetry (CV) measurements were conducted with a CHI660D electrochemical workstation in a deoxygenated dichloromethane solution of tetrabutylammoniunhexafluorophosphate (n-Bu_4NPF_6) under a nitrogen atmosphere (the concentration is 0.1 mol L^{-1}). A glassy carbon dish (working electrode) and platinum electrode (counter electrode) and Ag/AgCl electrode (reference electrode) were used. Measurements were carried out with ferrocene as the standard. The light sources were an FUV-6BK UV curing machine connected to LED irradiators of 365, 395, and 470 nm (Guangzhou Banwoo Electronic Technology Co., Ltd.). Near-infrared (NIR) spectroscopy was performed on a 5700 infrared spectrometer (Nicolet, USA) for analyzing the curing samples to detect the characteristic absorption peak change of the C═C double bond group for different (meth)acrylate resins with illumination time. DSC analyses were conducted on a DSC 200 F3 Maia (NETZSCH, Germany) at a heating rate of 10 °C/min under a nitrogen atmosphere. High-performance liquid chromatography (HPLC, Shimadzu, ProminenceLC-20A, Japan) and liquid

https://doi.org/10.1021/acsomega.1c02338
ACS Omega 2021, 6, 20902−20911

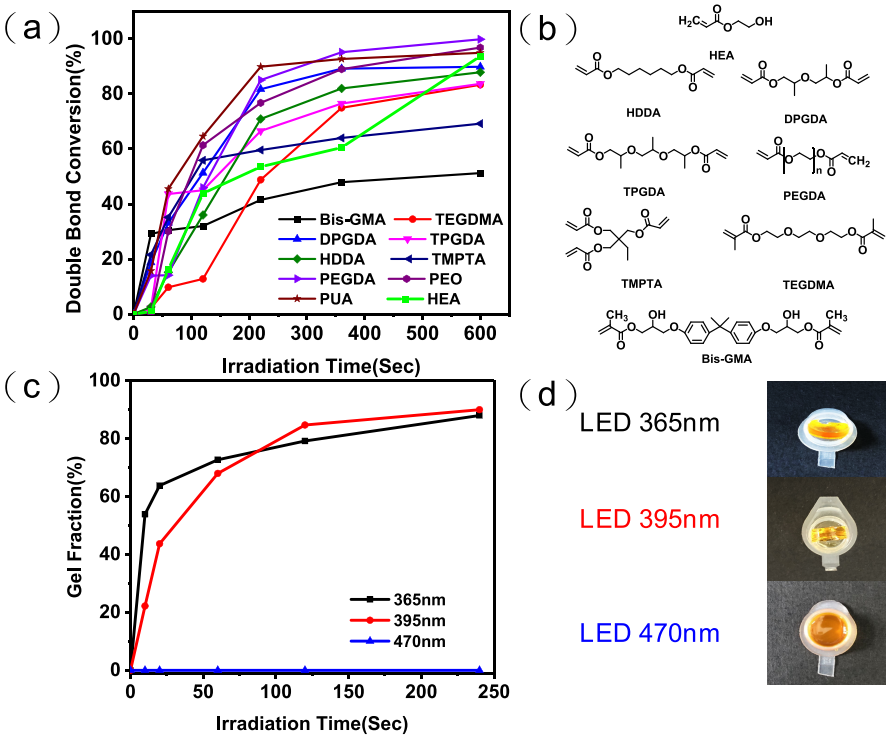

Figure 1. (a) Radical photopolymerization of 10 acrylate monomers and prepolymers using 0.5 wt % PyBN under LED irradiation at 365 nm. (b) Known chemical structures of the used acrylate monomers and prepolymers. (c) Gel fraction of 0.5 wt % PyBN/TMPTA under LED irradiation at 365, 395, and 470 nm. (d) Photos of the corresponding curing samples.

chromatography-mass spectroscopy (LC/MS, Shimadzu, LC/MS2020, Japan) were done for the study on the photolysis of PyBN.

2.3. Synthesis of PyBN. 4-Nitrobenzaldehyde (20 mmol, 3.02 g), 4-bromoaniline (20 mmol, 3.44 g), and *p*-toluene sulfonic acid (2 mmol, 0.38 g) were put into a two-necked bottle and then stirred in hydrous acetic acid of 25 mL at 90 °C for 0.5 h. Then, butane-2,3-dione (10 mmol, 0.86 g) was added and the resulting mixture was stirred at 90 °C for 3 h. After cooling, the precipitate was filtered and washed with glacial acetic acid. The pure product was obtained by recrystallization from ethyl acetate. PyBN: bright red solid, 2.3 g, yield: 30%. ^{1}H NMR (400 MHz, DMSO-d_6): δ 8.2 (d, J = 8.8 Hz, 2H), 7.7 (d, J = 8.7 Hz, 2H), 7.5 (d, J = 8.8 Hz, 2H), 7.3 (d, J = 8.6 Hz, 2H), 6.9 (s, 1H). ^{13}C NMR (101 MHz, chloroform-d): δ 145.8, 138.9, 138.1, 135.2, 133.6, 132.9, 127.9, 126.8, 124.0, 120.5, 97.1, 58.5, 18.5. HRMS (ESI) calcd. for $C_{30}H_{18}Br_2N_4O_4$ (M^+H^+): 657.9674, found:657.8799.

2.4. NIR Tests. The sample prepared was placed in a plastic round-hole mold with a diameter of 6 mm. An average value was determined from three repeated NIR tests. The light source was an LED curing machine with irradiators of different wavelengths. The optimized intensities of 365, 395, and 470 nm LED irradiators were 1.8, 38, and 110 mW cm^{-2}, respectively. The light intensities were measured using a single-channel UV-A illuminometer from the Beijing Normal University Optoelectronic Instrument Factory. The C═C double bond conversions of acrylate resins were calculated by detecting the characteristic absorption peak of double bond groups (at 6170 cm^{-1}) with illumination time.[39] Eq 1 is as follows:

$$\text{double bond conversion}\% = [1 - (S_T/S_0)] \times 100\% \quad (1)$$

where S_T is the area of the C═CH characteristic absorbance peak and S_0 is the initial area of the C═CH characteristic absorbance peak.

2.5. Steady-State Photolysis. The dichloromethane solution of PyBN was irradiated at intervals under LED irradiators of 365, 395, and 470 nm, respectively. The dichloromethane solution of CQ, CQ/EDBA, and CQ/PyBN was irradiated with an LED irradiator of 470 nm. Meanwhile, the LED irradiators were put above the solution at a fixed height of 4.0 cm.

3. RESULTS AND DISCUSSION

3.1. Radical Photopolymerization of PyBN/Acrylate Systems. First, the photopolymerization of different PyBN/acrylate systems in laminate was investigated using the NIR method with LED irradiation at 365 nm and a light intensity of 1.8 mW cm^{-2}. The thickness of the samples in laminate is 120 μm. PyBN (0.5 wt %) can effectively initiate the photopolymerization of acrylate monomers (Bis-GMA, TEGDMA, hydroxyethyl acrylate (HEA), DPGDA, TPGDA, HDDA, and TMPTA) and prepolymers (PEGDA, PEO, and PUA), implying that PyBN can act as an efficient photoinitiator in these curing systems. NIR results showing the double bond conversion induced by PyBN in the 10 acrylate resins upon LED irradiation at 365 nm are exhibited in Figure 1a. The chemical structures of the used acrylate monomers and prepolymers are shown in Figure 1b. The double bond conversion of the 0.5 wt % PyBN/HEA system upon 365 nm LED irradiation is >90% after 360 s. The high double bond conversion is in accordance with the literature reports describing monofunctional acrylate monomers, confirming that the initiating species is successfully generated from PyBN as the photoinitiator[40,41] Additionally, a high double

https://doi.org/10.1021/acsomega.1c02338
ACS Omega 2021, 6, 20902−20911

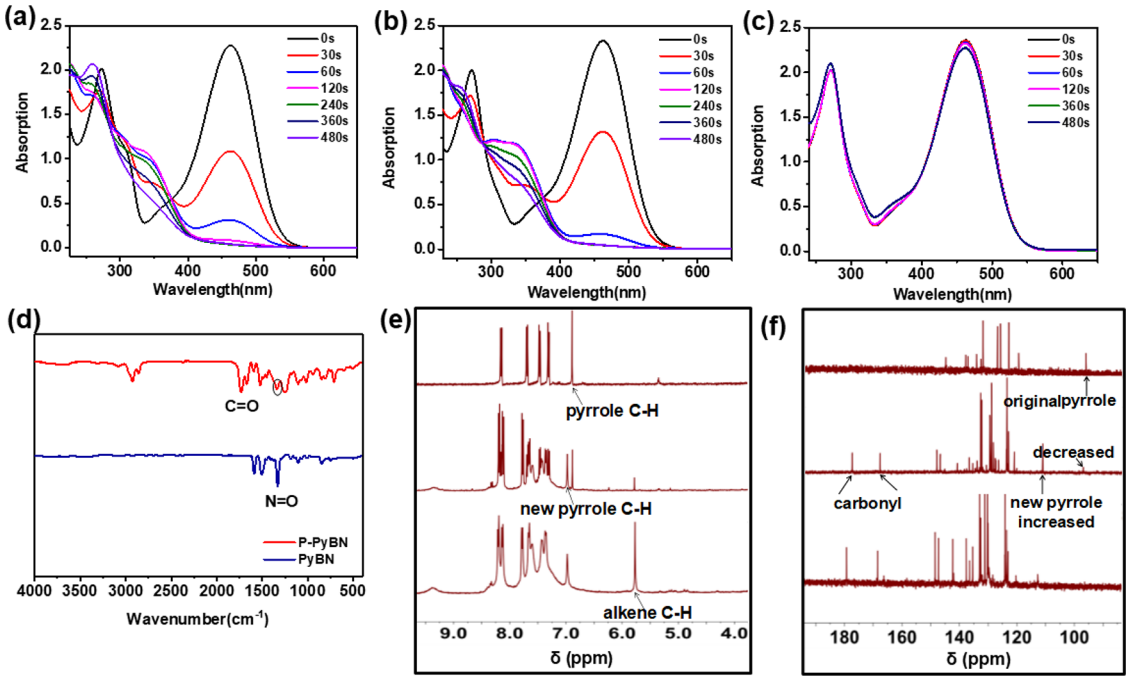

Figure 2. Photolysis of PyBN of 5×10^{-6} mol L^{-1} in CH_2Cl_2 under LED irradiation at (a) 365 nm, (b) 395 nm, and (c) 470 nm analyzed by UV−visible spectroscopy. Comparison of the (d) IR, (e) ^{1}H NMR, and (f) ^{13}C NMR data of PyBN before and after LED irradiation at 365 nm.

bond conversion of up to 99.86% is achieved for PyBN/PEGDA.

The photographs of both pure HEA and PYBN/HEA after irradiation are shown in Figure S1a. After irradiation for 360 s, the product obtained after the photopolymerization of monofunctional HEA using PyBN upon irradiation at 365 nm becomes less soluble and swells in tetrahydrofuran (THF). This product was analyzed in detail by NMR (Figures S2 and S3). The changes in the 0.5−2 ppm region of the ^{1}H NMR spectra upon conversion from pure HEA to PYBN/HEA after irradiation indicate that the resultant carbon-centered radicals probably act as the cross-linking agents and form new alkyl groups during the cross-linking process.[42] Figure S1b,c show the DSC curves of the first and second cycles of PyBN/HEA at 0 s and after irradiation with 365 nm LED for 360 s, respectively. The maximal heat flow of the exothermic peak at 360 s decreases in comparison to that at 0 s. The exothermic peak is mainly attributed to the autopolymerization of the residual acrylate monomers at an onset temperature of 100 °C. Similarly, the DSC thermograms for the photopolymerized samples of PyBN/PEGDA and PyBN/TMPTA were obtained for comparison (Figure S4). The exothermic peaks of PyBN/TMPTA result from the autopolymerization of the residual acrylate monomers with an increase in temperature as TMPTA is a multifunctional acrylate monomer yielding a lower double bond conversion than PEGDA.[43] The DSC results confirm that the polymerization reactions occur, which are consistent with the NIR data shown in Figure 1a. These results indicate that both the acrylate monomers and prepolymers show high cross-linking upon irradiation with 365 nm LED within 600 s. Thus, the PyBN system is effective for radical photopolymerization.

Since TMPTA is a highly reactive radical monomer, the polymerization of PyBN/TMPTA by the gel fraction method was further evaluated. The gel fraction results show that the PyBN/TMPTA system affords a curing conversion of 88.0% upon irradiation at 365 nm and 90.0% at 395 nm; TMPTA does not polymerize at 470 nm (Figure 1c). PyBN (0.5 wt %) is used, and the samples for the gel fraction method are used without any treatment and simply dropped on a slide glass in air. The thickness of samples in air is 400 μm. For irradiation at 395 nm, the initial polymerization of PyBN/TMPTA is slower than that at 365 nm when the irradiation time is less than 100 s. After 100 s, the polymerization accelerates, affording a competitive performance. From Figure 1d, the curing products of PyBN/TMPTA under LED irradiation at 365 and 395 nm include a suitably cross-linked polymer in the solid state. The sample of PyBN/TMPTA does not polymerize under irradiation at 470 nm and remains liquid. As mentioned in Section 2.4, the light intensities of 365, 395, and 470 nm of our LED irradiators are optimized to be 1.0, 38, and 110 mW cm^{-2}, respectively. When at the same light intensity of 1.8 mW cm^{-2}, NIR data reveal that PyBN has a superior initiating activity under LED irradiation at 365 nm compared with 395 and 470 nm (Figure S5). The photoinitiating efficiency increased until a light intensity of 395 nm up to the highest value of 38 mW cm^{-2}. However, for 470 nm LED, the increase in light intensity reaching the highest 110 mW cm^{-2} still did not work.

To further evaluate the effectiveness of the photoinitiating capability of different 1,4-dihydropyrrolo[3,2-*b*]pyrrole derivatives, 1,4-bis(4-bromophenyl)-2,5-di-*p*-tolyl-1,4-dihydropyrrolo[3,2-*b*]pyrrole (PyBC) was prepared as a reference compound. The synthetic route of PyBC is shown in Scheme S1. The photopolymerization of TMPTA formulated with PyBC (0.5 wt %) was examined by the same gel fraction method mentioned previously (Figure S6). Under LED irradiation at 365 and 395 nm, conversion values of 94.1 and 35.2%, respectively, are obtained during curing, whereas negligible polymerization is observed at 470 nm. This is mainly owing to the shorter absorption wavelength range for PyBC than that for PyBN, as shown in Figure S7. The

https://doi.org/10.1021/acsomega.1c02338
ACS Omega 2021, 6, 20902−20911

corresponding parameters are listed in Table S1. Therefore, 1,4-dihydropyrrolo[3,2-*b*]pyrrole derivatives are excellent candidates for use as highly efficient photoinitiators in radical photopolymerization. Nitro-based PyBN has advantages in long-wavelength polymerization at 395 nm compared to the methyl-based PyBC because of its extended absorption band range.

3.2. Photolysis of PyBN. Considering the wavelength-selective properties of PyBN, the photolysis of PyBN was studied under LED irradiation at different wavelengths. The ultraviolet−visible (UV−vis) spectra of PyBN in dichloromethane at a concentration of 5×10^{-6} mol L^{-1} were obtained at increasing irradiation times (Figure 2a−c). Interestingly, the major maximum absorption peak is observed at 462 nm, while an additional absorption peak is observed at 271 nm. In CH_2Cl_2 solution, the two absorption peaks at around 271 and 462 nm (Figure 2a) can be assigned as the $\pi-\pi*$ transitions of the nitro groups and the pyrrolo[3,2-*b*]pyrrole core, respectively, and the broad absorption band at 462 nm corresponds to the intramolecular charge transfer (ICT) transition from the pyrrolo[3,2-*b*]pyrrole core to the peripheral nitro units.[44]

During steady-state photolysis, the absorption peak at 462 nm significantly blueshifts to 300−400 nm, affording a shoulder peak when irradiated at either 365 or 395 nm. Similarly, the absorption peak at 271 nm also blueshifts to afford a new shoulder peak. In contrast, PyBN shows almost no bleaching behavior at 470 nm in contrast to that at 365 and 395 nm. The steady-state photolysis result is consistent with the polymerization performance monitored by NIR spectroscopy. NIR results show that PyBN does not work as a photoinitiator at 470 nm, which can indicate that at 470 nm, there is not enough energy to create the active radical species due to its strong ICT property and that only at higher energy transitions can the radical necessary to initiate the photopolymerization be provided. In Figure S8, the UV−vis absorption bands of PyBN in DMF, DMSO, CH_2Cl_2, and CH_3CN with different polarities were investigated. The absorption wavelength of PyBN increased in an order of CH_3CN (454 nm) < CH_2Cl_2 (462 nm) < DMF (468 nm) < DMSO(472 nm). The positive solvatochromic (bathochromic shift) character upon the increase in solvent polarity demonstrates strong intramolecular charge transfer ability.[45] Thus, rapid photolysis is beneficial for PyBN to exhibit good initiation in acrylate-based radical photopolymerization systems.

The photolysis of PyBN to yield transformation products was first analyzed by thin layer chromatography (Figure S9). With a decrease in the amount of PyBN, new products with high polarity are observed. IR and NMR spectroscopy were done to monitor the structural changes in PyBN upon irradiation. Figure 2d shows the change in the IR data of PyBN before and after light irradiation for 320 s. After LED irradiation at 365 nm, the intensities of the original characteristic peaks of N=O at 1595.5 and 1320 cm^{-1} decrease significantly. New peaks at 1730 and 1669 cm^{-1} that can be attributed to C=O stretching are observed. The ^1H NMR and ^{13}C NMR spectra were recorded to further analyze the products. As shown in Figure 2e, the ^1H NMR spectrum of PyBN shows a peak at 6.88 ppm, corresponding to the C−H of pyrrole, and a new peak at 6.99 ppm is observed after irradiation for 320 s. This indicates the formation of a new pyrrole[3,2-*b*]pyrrole structure. The peak at 5.75 ppm corresponds to the C−H of the alkene moiety generated after irradiation for 480 s. As shown in Figure 2f, the ^{13}C NMR spectrum shows peaks at 178.3 and 168.7 ppm for 320 and 480 s, confirming the presence of C=O groups, respectively. The increased signal of peaks at 130−150 ppm is attributed to the carbon of the alkene moiety, which is consistent with the ^1H NMR data. The chemical shifts of the two signals observed in the ^{13}C NMR spectra are between 160 and 190 ppm, which result from a chemical reaction or transformation of the C=O group of the photolysis product. The full-scale NMR spectra are shown in Figures S18−S23. Based on these data, carbonyl radicals are probably generated from the photoinitiation by PyBN. Carbonyl radicals are the key to induce radical photopolymerization.

Electron paramagnetic resonance (EPR) was used to detect the carbonyl radicals formed by PyBN. The EPR spectra of the radicals generated upon irradiation are shown in Figure 3. The

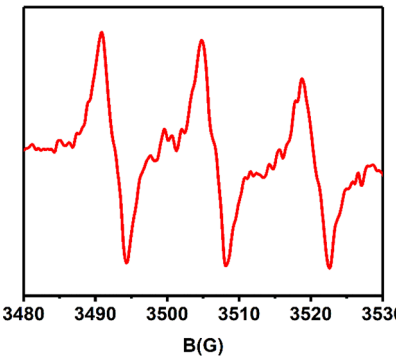

Figure 3. EPR spectra obtained after the irradiation of a *tert*-butylbenzene (PBN) solution of PyBN/PBN at 365 nm under argon for 480 s. The light intensity is 1.8 mW cm^{-2}, and the concentrations of PyBN and PBN are 5×10^{-5} and 5×10^{-2} mol L^{-1}, respectively.

radicals generated in the form of radical adducts with the spin trapping agent (phenyl-*N*-tert-butylnitrone (PBN)) can be detected when the PyBN/PBN solution is subjected to a 365 nm LED irradiation. The radical adducts are confirmed by the hyperfine coupling constants (a_N = 13.9 G, a_H = 3.4 G) of the EPR experimental spectra, which are consistent with those reported in the literature.[5]

Based on the IR, NMR, and EPR data, a possible mechanism for inducing radical photopolymerization by PyBN is shown in Scheme S2. As compared, PyBN was consumed and new product was generated. The nitro (NO_2)-to-carbonyl conversion is the main transformation during the photolysis of PyBN, based on reported studies.[46−49] The generated phenoxy radicals can first undergo a rearrangement to form the carbonyl radical.[47,48] The carbonyl radical can induce the polymerization of the acrylate monomer. Thus, the pyrrolo[3,2-*b*]pyrrole-based PyBN can efficiently initiate radical polymerization upon irradiation at 365 and 395 nm. The HPLC and LC/MS methods were conducted for further demonstrating the occurrence of the photolysis process and analyzing the obtained products (Figures S24−S26). The retention time in detail are listed in Tables S2 and S3. LC/MS results further indicate that the reaction outlined in Scheme S2 could take place. In reversed-phase chromatographic columns, a main photolysis product is that with shorter retention time at 18.502 min (Figure S25 and Table S3), which is inconsistent with the result in Figure S10 that the photolysis product has larger

https://doi.org/10.1021/acsomega.1c02338
ACS Omega 2021, 6, 20902−20911

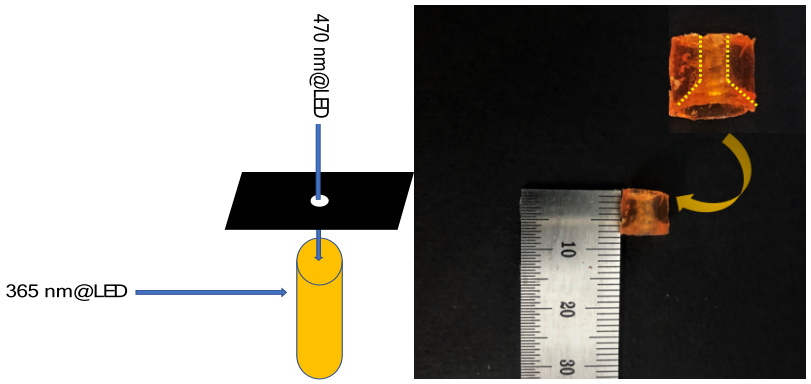

Figure 4. Sample after being cured by dual-wavelength photopolymerization.

polarity than PyBN. The retention time of PyBN is at 22.818 min, as shown in Figure S24 and Table S2. The molecular weight (MW) of the original PyBN is 658 g mol^{-1} ($C_{30}H_{18}Br_2N_4O_4$). Thus, the MW of the main product as inferred in Scheme S2 is 596 g mol^{-1} ($C_{30}H_{18}Br_2N_2O_2$). The peak of the main product at m/z = 542 possibly represents its fragment of $C_{28}H_{20}Br_2N_2$, which might point to the fracture from C6 to C5. The inferred structure of this photolysis product is given as Figure S27.

The EPR spectra of the PyBN/PBN solution subjected to a 470 nm LED irradiation are investigated, as shown in Figure S10. Figure S10a,b are tested under the same condition using the same power as that upon a 365 nm LED irradiation of 2 mW. No radical adducts were observed upon irradiation of 470 nm LED for 240 s (Figure S10a) and even when the irradiation time was increased to 800 s (Figure S10b). Upon greatly enhancing the power to 6.325 mW, the radical adducts with the similar hyperfine coupling constants (a_N = 13.8 G, a_H = 1.2 G) emerged (Figure S10c).[50] This result explains that the rapid initiation in a short time with 365 nm LED irradiation is mainly due to the formation of a high concentration of carbonyl radicals from PyBN. However, during the same period, the concentration of free radicals produced by PyBN with 470 nm LED irradiation did not reach the threshold value to induce polymerization. Maybe a new 470 nm LED light source with a large intensity is needed for a future study on the photochemical properties of PYBN.

3.3. Dual-Wavelength Photopolymerization of PyBN/TMPTA for Volumetric Additive Manufacturing. One of the applications expected for PyBN is volumetric additive manufacturing, which is based on the concurrent dual-wavelength irradiation. One wavelength is used for photoinitiation, and the other is for photoinhibition. Dual-wavelength curing for a volumetric photopolymerization system is beneficial for printing 3D structures by only single exposure in comparison to the layer-by-layer 3D printing techniques. The dual-wavelength curing of TMPTA in the presence of 0.5 wt % PyBN was investigated. Based on the reports,[13,14,31] one wavelength is used to induce photopolymerization and second wavelength to interfere with photopolymerization. The resin was irradiated using two concurrent wavelengths, both of which included simultaneous LED irradiation at 365 and 470 nm in two directions. The purpose of the second independent wavelength of 470 nm light is to significantly reduce the concentration of active radicals, and thus the rate of polymerization is also reduced under co-irradiation, thereby the 470 nm LED is an interferent for the photopolymerization process. This is a two-color (UV and blue) photo-orthogonal irradiation scheme.[31] This scheme is a two-color pattern commonly used in direct writing lithography.[51] Only one wavelength cannot get the desired performance. The corresponding schematic diagram is given in Figure 4. The original product obtained from the hose slot is shown in Figure S11. The 365 nm light was rotated (360°) around the sample. The 470 nm light passed through a circular aperture mask and was stationary. A hollow structure was then directly fabricated, which cannot be obtained with only 365 nm and without 470 nm (Figure S12). The middle hollow part is created by no cross-linking owing to the interference of the 470 nm light. Although PyBN does not show photolysis at 470 nm and no radicals were generated during the fast irradiation period upon 365 nm light (as shown in Figure S10), the ground-state PyBN may shift to a lower excited state via the highest occupied molecular orbital (HOMO)−lowest occupied molecular orbital (LUMO) transition after absorbing 470 nm light. Meanwhile, PyBN shifts to a higher excited state upon 365 nm irradiation. Thus, PyBN at the higher excited state can be consumed by the lower excited state in the region irradiated by 470 nm light due to its ICT property.[26] The funnel-shaped product is attributed to the beam shape of 470 nm light. The de-excitation of PyBN in the high excitation state before intersystem crossing to the triplet state for radical generation is a key step that hinders photopolymerization. The fast generation of enough active radicals with under 365 nm light is an important factor to accomplish this application. At this short period, the 470 nm light interferes with PyBN to get a low-excited state instead of radical generation. Therefore, only 365 nm cannot result in a unique hollow product. This study indicates that PyBN is a promising candidate for volumetric additive manufacturing.

3.4. Visible-Light-Induced Radical Photopolymerization Initiated by CQ and PyBN. Interestingly, PyBN can also interact well with the visible-light photoinitiator, CQ. PyBN affords a maximum absorption peak, which is close CQ, but shows a much stronger maximum molar extinction coefficient (ε_{max}), as indicated by Figure S7 and Table S1. CQ/PyBN was investigated as a two-component photoinitiating system for TMPTA under LED irradiation at 470 nm. To gain insights into the electronic properties of PyBN, theoretical calculations by density functional theory at the B3LYP/6-31G (g, d) level were performed. The photoelectron transfer (PET) between CQ and PyBN was evaluated based on the calculation of the Rehm−Weller equation.[39]

https://doi.org/10.1021/acsomega.1c02338
ACS Omega 2021, 6, 20902−20911

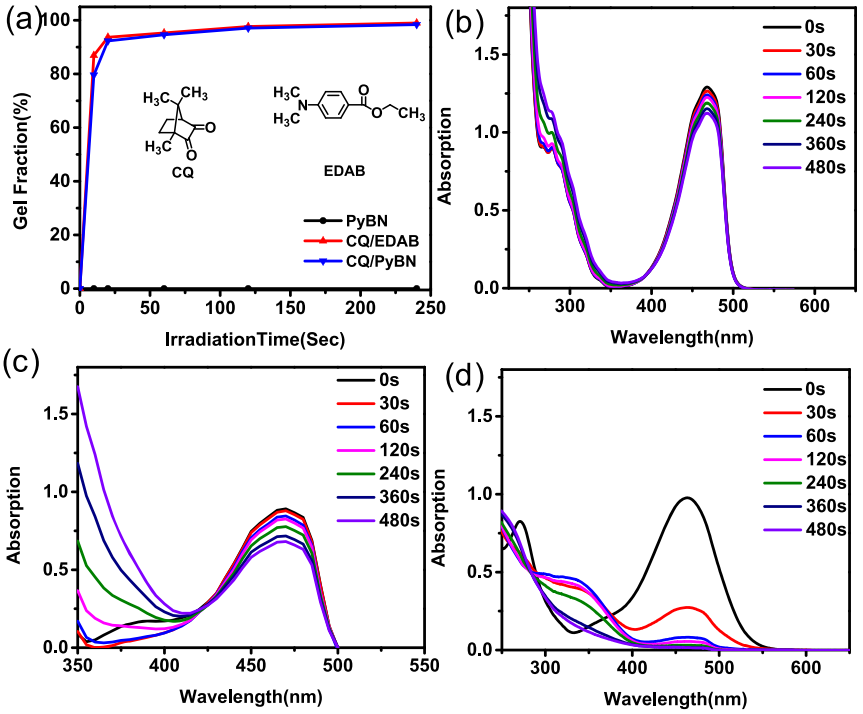

Figure 5. (a) Gel fraction results of photoinduced 0.5 wt % PyBN/TMPTA, 1.0 wt % CQ/0.5 wt % EDAB/TMPTA, and 1.0 wt % CQ/0.5 wt % PyBN/TMPTA upon irradiation at 365, 395, and 470 nm. The photolysis for (b) CQ of 3×10^{-3} mol L^{-1}, (c) CQ/EDAB mixture with concentrations of 3×10^{-3} and 2×10^{-3} mol L^{-1}, and (d) CQ/PyBN mixture with concentrations of 3×10^{-3} and 5×10^{-6} mol L^{-1} under 470 nm LED irradiation.

The excellent absorption properties of PyBN are associated with the large delocalization of the HOMO and LUMO. As shown in Figure S13, the HOMO of PyBN is localized on the entire skeleton bearing the nitro groups. The LUMO of PyBN shows the electron-withdrawing effect of the nitro group, pulling electrons from the pyrrolo[3,2-*b*]pyrrole core. The push−pull structure enlarges the conjugation plane. The excellent light absorption properties of PyBN can be attributed to the $\pi-\pi^*$ transition of the entire π-conjugated structure, resulting in the promotion of charge transfer.

Furthermore, the synergistic effect of CQ and PyBN is demonstrated by investigating the spectroscopic and electrochemical behaviors of the CQ/PyBN two-component system. The free energy change (ΔG_{el}) for the PET between the excited state of PyBN as an electron donor and CQ as an electron acceptor is calculated. Owing to the higher molar extinction coefficient of PyBN at 470 nm than that of CQ, PyBN possibly first absorbs a photon to attain the excited state. The CV results afford the oxidation potential (E_{ox}) of the electron donor (PyBN) and reduction potential (E_{red}) of the electron acceptor (CQ) (Figure S14). The reduction potential of CQ is −1.064 V, determined in a separate experiment, and the oxidation potential of PyBN is −0.998 V. The singlet excited state energy (E_{00}) of PyBN is calculated as 2.40 eV from the intersection wavelength of its absorption and emission spectra (Figure S15). The calculated ΔG_{el} for the CQ/PyBN photoredox pair is −2.33 eV, which indicates that its PET is thermodynamically allowed. The E_{ox} and E_{00} values of PyBC are −0.556 and 3.1 eV, respectively. The calculated ΔG_{el} for the CQ/PyBC photoredox pair is also negative (−2.59 eV) based on Figures S14 and S15. These results suggest that in addition to the nitro-based 1,4-dihydropyrrolo-[3,2-*b*]pyrrole derivatives, the interactions of other substituted 1,4-dihydropyrrolo[3,2-*b*]pyrrole molecules with CQ should also be investigated.

CQ is typically used with EDAB as a suitable two-component photoinitiator for visible-light-induced radical photopolymerization. By the addition of EDAB, which is a tertiary amine, more efficient photopolymerization than that of CQ is observed. In this study, PyBN is demonstrated to show a good interaction with CQ under LED irradiation at 470 nm. The photopolymerization of TMPTA in the presence of CQ/PyBN was performed in air, and a similar CQ/EDAB system was also studied for comparison. The corresponding gel fraction results are shown in Figure 5a. CQ/PyBN can effectively initiate the photopolymerization of TMPTA to achieve almost complete curing at 470 nm with a similar efficiency to that of CQ/EDAB. PyBN shows no initiation capability at 470 nm, as discussed in Section 3.1. This result indicates that CQ and PyBN show a synergistic effect during photoinitiation. Similarly, CQ/PyBC initiates TMPTA to afford a high curing conversion (Figure S16).

Furthermore, the photolysis of CQ, CQ/EDAB, and CQ/PyBN in solution was investigated (Figure 5b−d). The maximum absorption peak of CQ/EDAB shows a new, more redshifted shoulder at 350−400 nm relative to that of CQ at 250−300 nm. The maximum absorption of CQ/PyBN under 470 nm LED irradiation decreases rapidly, in contrast to the photolysis of PyBN at 470 nm, as described in Section 3.1. Consequently, the reaction between CQ and PyBN is effective.

As shown in Figure S17, the fluorescence intensities of the CQ solution (1×10^{-4} mol L^{-1}) in the absence and presence of PyBN with different concentrations of 7.6×10^{-5} and 1.1×10^{-4} mol L^{-1} are measured. The maximum fluorescence emission at 512 nm is attributed to CQ, which can be significantly quenched by the addition of PyBN. The maximum

https://doi.org/10.1021/acsomega.1c02338
ACS Omega 2021, 6, 20902−20911

fluorescence emission wavelength of PyBN is 568 nm, as determined experimentally in our lab. Thus, the synergistic effect between CQ and PyBN is further confirmed.

4. CONCLUSIONS

A 1,4-dihydropyrrolo[3,2-*b*]pyrrole derivative, 1,4-bis (4-bromophenyl)-2,5-bis (4-nitrophenyl)-1,4-dihydropyrrole[3,2-*b*]pyrrole (PyBN), is synthesized in this study. Owing to its good wavelength-selective properties, it is employed as a photoactive component in the radical photopolymerization systems irradiated using an LED lamp. Upon irradiation at wavelengths of 365 and 395 nm, PyBN can be used as a one-component photoinitiator, which successfully initiates the polymerization of nine different (meth)acrylate materials. The double bond conversion is analyzed by both NIR data and gel fraction method, affording the highest conversion of up to 99.86% under low-intensity light. This result indicates that PyBN can be employed as a novel 365 and 395 nm radical photoinitiator. Although PyBN shows the maximum visible light absorption at 462 nm (which is close to 470 nm) upon irradiation at 470 nm, it barely shows photolysis but can interact with CQ to form a two-component visible-light photoinitiator system. Upon irradiation using identical light intensity, the CQ/PyBN system is demonstrated to afford a similar efficiency to that of CQ/EDAB, which is an efficient co-initiator for CQ. Therefore, PyBN is a multifunctional photoinitiator and co-initiator for radical photopolymerization upon irradiation at different wavelengths. Notably, PyBN is also useful for volumetric additive manufacturing. New 1,4-dihydropyrrolo[3,2-*b*]pyrrole derivatives need to be prepared to explore structure−property relationships in the future.

■ ASSOCIATED CONTENT

Supporting Information

The Supporting Information is available free of charge at https://pubs.acs.org/doi/10.1021/acsomega.1c02338.

Electron paramagnetic resonance (EPR) experiments' spectrometer parameters; synthesis of 1,4-bis(4-bromophenyl)-2,5-di-*p*-tolyl-1,4-dihydropyrrolo[3,2-*b*]pyrrole (PyBC); DSC curves of PyBN/HEA, PyBN/PEGDA, and PyBN/TMPTA systems; EPR spectra at 470 nm; NIR, DSC, and NMR of PyBN/HEA; gel fraction of PyBC/TMPTA; absorption spectra of PyBC, PyBN, and CQ; thin layer chromatography of PyBN and after photolysis; possible mechanism for inducing radical photopolymerization by PyBN; sample after being cured by dual-wavelength photopolymerization; frontier molecular orbital distributions of PyBN; CV curves of PyBN, PyBC, and CQ; normalized absorption and emission spectra of PyBN and PyBC; gel-fraction result of CQ/PyBC/TMPTA under an LED irradiator of 470 nm in air; fluorescence emission spectra of CQ and CQ/PyBN; ^{1}H NMR and ^{13}C NMR spectra of PyBN and after irradiation; and HPLC and LC/MS of PyBN after irradiation of 365 nm LED for 480 s (PDF)

■ AUTHOR INFORMATION

Corresponding Author

Yu Chen − *Tianjin Key Laboratory of Organic Solar Cells and Photochemical Conversion, Tianjin Key Laboratory of Drug Targeting and Bioimaging, Department of Applied Chemistry, School of Chemistry and Chemical Engineering, Tianjin University of Technology, Tianjin 300384, People's Republic of China*; orcid.org/0000-0003-4138-260X; Email: chenyu18417@email.tjut.edu.cn

Authors

Yuanyuan Xu − *Tianjin Key Laboratory of Organic Solar Cells and Photochemical Conversion, Tianjin Key Laboratory of Drug Targeting and Bioimaging, Department of Applied Chemistry, School of Chemistry and Chemical Engineering, Tianjin University of Technology, Tianjin 300384, People's Republic of China*

Xuguang Liu − *Tianjin Key Laboratory of Organic Solar Cells and Photochemical Conversion, Tianjin Key Laboratory of Drug Targeting and Bioimaging, Department of Applied Chemistry, School of Chemistry and Chemical Engineering, Tianjin University of Technology, Tianjin 300384, People's Republic of China*; orcid.org/0000-0002-7859-3139

Song Xue − *Tianjin Key Laboratory of Organic Solar Cells and Photochemical Conversion, Tianjin Key Laboratory of Drug Targeting and Bioimaging, Department of Applied Chemistry, School of Chemistry and Chemical Engineering, Tianjin University of Technology, Tianjin 300384, People's Republic of China*

Complete contact information is available at: https://pubs.acs.org/10.1021/acsomega.1c02338

Author Contributions

The manuscript was written through contributions of all authors. All authors have given approval to the final version of the manuscript.

Notes

The authors declare no competing financial interest.

■ ACKNOWLEDGMENTS

The authors gratefully thank the financial support of the Natural Science Foundation of Tianjin City (17JCZDJC37700 and 18JCZDJC97000).

■ REFERENCES

(1) Norouzbahari, S.; Gharibi, R. UV Cross-Linked Poly (ethylene glycol)-Based Membranes with Different Fractional Free Volumes for CO_2 Capture: Synthesis, Characterization, and Thiolene Modification Evaluation. *Ind. Eng. Chem. Res.* **2020**, *13*, 6078−6089.

(2) Bagheri, A.; Jin, J. Photopolymerization in 3D Printing. *ACS Appl. Polym. Mater.* **2019**, *1*, 593−611.

(3) Zhang, M.; Jiang, S.; Gao, Y.; Nie, J.; Sun, F. UV-Nanoimprinting Lithography Photoresists with No Photoinitiator and Low Polymerization Shrinkage. *Ind. Eng. Chem. Res.* **2020**, *16*, 7564−7574.

(4) Argine, C. D.; Hochwallner, A.; Klikovits, N.; Liksa, R.; Stampf, J.; Sangermano, M. Hot-lithography SLA-3D printing of epoxy resin. *Macromol. Mater. Eng.* **2020**, *305*, 2000325.

(5) Ma, X.; Cao, D.; Hu, X.; Nie, J.; Wang, T. Carbazolyl α-diketones as novel photoinitiators in photopolymerization under LEDs. *Prog. Org. Coat.* **2020**, *144*, 105651.

(6) Lee, K. S.; Kim, R. H.; Yang, D. Y.; HuPark, S. Advances in 3D nano/microfabrication using two-photon initiated polymerization. *Prog. Polym. Sci.* **2008**, *33*, 631−681.

(7) Weems, A. C.; Delle Chiaie, K. R.; Yee, R.; Dove, A. P. Selective reactivity of myrcene for vat photopolymerization 3D printing and postfabrication surface modification. *Biomacromolecules* **2020**, *21*, 163−170.

(8) Eibel, A.; Fast, D. E.; Sattelkow, J.; Zalibera, M.; Wang, J.; Huber, A.; Müller, G.; Neshchadin, D.; Dietliker, K.; Plank, H.; Grützmacher, H.; Gescheidt, G. Star-shaped polymers through simple

wavelength-selective free-radical photopolymerization. *Angew. Chem. Int. Edit.* **2017**, *56*, 14306−14309.
(9) Tang, L.; Nie, J.; Zhu, X. A high performance phenyl-free LED photoinitiator for cationic or hybrid photopolymerization and its application in LED cationic 3D printing. *Polym. Chem.* **2020**, *11*, 2855−2863.
(10) Bagheri, A.; Bainbridge, C. W. A.; Engel, K. E.; Qiao, G. G.; Xu, J.; Boyer, C.; Jin, J. Oxygen tolerant PET-RAFT eacilitated 3D printing of polymeric materials under visible LEDs. *ACS Appl. Polym. Mater.* **2020**, *2*, 782−790.
(11) Yu, C.; Schimelman, J.; Wang, P.; Miller, K. L.; Ma, X.; You, S.; Guan, J.; Sun, B.; Zhu, W.; Chen, S. Photopolymerizable biomaterials and light-based 3D printing strategies for biomedical applications. *Chem. Rev.* **2020**, *120*, 10695−10743.
(12) Hong, S. Y.; Kim, Y. C.; Wang, M.; Kim, H. I.; Suhr, J. Experimental investigation of mechanical properties of UV-curable 3D printing materials. *Polymer* **2018**, *145*, 88−94.
(13) Beer, M. P.; Laan, H. L.; Cole1, M. A.; Whelanl, R. J.; Burns, M. A.; Scott, T. F. Rapid, continuous additive manufacturing by Avolumetric polymerization inhibition patterning. *Sci. Adv.* **2019**, *5*, 8723.
(14) Loterie, D.; Delrot, P.; Moser, C. High-resolution tomographic volumetric additive manufacturing. *Nat. Commun.* **2020**, *11*, 852.
(15) Ligon, S. C.; Liska, R.; Stampf, J.; Gurr, M.; Mülhaupt, R. Polymers for 3D printing and customized additive manufacturing. *Chem. Rev.* **2017**, *117*, 10212−10290.
(16) Mousawi, A. A.; Garra, P.; Sallenave, X.; Dumur, F.; Toufaily, J.; Hamieh, T.; Graff, B.; Gigmes, D.; Fouassier, J. P.; Lalevée, J. π-Conjugated dithienophosphole derivaives as high performance photoinitiators for 3D printing resins. *Macromolecules* **2018**, *51*, 1811−1821.
(17) Zhang, X. Q.; Keck, S.; Qi, Y. J.; Baudis, S.; Zhao, Y. X. Study on modified dealkaline lignin as visible light macromolecular photoinitiator for 3D printing. *ACS Sustainable Chem. Eng.* **2020**, *8*, 10959−10970.
(18) Shao, J.; Huang, Y.; Fan, Q. Visible light initiating systems for photopolymerization: status, development and challenges. *Polym. Chem.* **2014**, *5*, 4195−4210.
(19) Ding, R.; Du, Y. Y.; Goncalves, R. B.; Francis, L. F.; Reineke, T. M. Sustainable near UV-curable acrylates based on natural phenolics for stereolithography 3D printing. *Polym. Chem.* **2019**, *10*, 1067−1077.
(20) Steyrer, B.; Busetti, B.; Harakály, G.; Liska, R.; Stampfl, J. Hot Lithography vs. room temperature DLP 3D-printing of a dimethacrylate. *Addit. Manuf.* **2018**, *21*, 209−214.
(21) Gauss, P.; Griesser, M.; Markovic, M.; Ovsianikov, A.; Gescheidt, G.; Knaack, P.; Liska, R. α-Ketoesters as Nonaromatic Photoinitiators for Radical Polymerization of (Meth)acrylates. *Macromolecules* **2019**, *52*, 2814−2821.
(22) Borrello, J.; Nasser, P.; Iatridis, J. C.; Costa, K. D. 3D printing a mechanically-tunable acrylate resin on a commercial DLP-SLA printer. *Addit. Manuf.* **2018**, *23*, 374−380.
(23) Guit, J.; Tavares, M. B. L.; Hul, J.; Ye, C.; Loos, K.; Jager, J.; Folkersma, R.; Voet, V. S. D. Photopolymer resins with biobased methacrylates based on soybean oil for stereolithography. *ACS Appl. Polym. Mater.* **2020**, *2*, 949−957.
(24) Branciforti, D. S.; Lazzaroni, S.; Milanese, C.; Castiglioni, M.; Dondi, D. Visible light 3D printing with epoxidized vegetable oils. *Addit. Manuf.* **2019**, *25*, 317−324.
(25) Voet, V. S. D.; Orcid; Strating, T.; Schnelting, G. H.; Dijkstra, P.; Tietema, M.; Xu, J.; Woortman, A. J.; Orcid, K. L.; Jager, J.; Folkersma, R. Biobased acrylate photocurable resin formulation for stereolithography 3D printing. *ACS Omega* **2018**, *3*, 1403−1408.
(26) Li, L.; Gattass, R. R.; Gershgoren, E.; Hwang, H.; Fourkas, J. T. Achieving λ/20 resolution by one-color initiation and deactivation of polymerization. *Science* **2009**, *324*, 910.
(27) Cameron, N. R.; Lagrille, O.; Lovell, P. A.; Thongnuanchan, B. A nitroxide for effecting controlled nitroxide-mediated radical polymerization at temperatures ≤90 °C. *ACS Macro Lett.* **2012**, *1*, 1262−1265.
(28) Sautrot-Ba, P.; Jockusch, S.; Malval, J. P.; Brezová, V.; Rivard, M.; Andaloussi, S. A.; Grzechnik, A. B.; Versace, D. L. Quinizarin derivatives as photoinitiators for free-radical and cationic photopolymerizations in the visible spectral range. *Macromolecules* **2020**, *53*, 1129−1141.
(29) Breloy, L.; Brezova, V.; Grzechnik, A. B.; Presset, M.; Yildirim, M. S.; Yilmaz, I.; Yagci, Y.; Versace, D. L. Visible light anthraquinone functional phthalocyanine photoinitiator for free-radical and cationic polymerizations. *Macromolecules* **2020**, *53*, 112−124.
(30) Liao, W.; Xu, C.; Wu, X.; Liao, Q.; Xiong, Y.; Li, Z.; Tang, H. Photobleachable cinnamoyl dyes for radical visible photoinitiators. *Dyes Pigm.* **2020**, *178*, 108350.
(31) Laan, H. L.; Burns, M. A.; Scott, T. F. Volumetric photopolymerization confinement through dual-wavelength photoinitiation and photoinhibition. *ACS Macro Lett.* **2019**, *8*, 899−904.
(32) Janiga, A.; Gryko, D. T. 1,4-Dihydropyrrolo[3,2-b]pyrrole and its p-expanded analogues. *Chem. − Asian J.* **2014**, *9*, 3036−3045.
(33) Ji, Y.; Peng, Z.; Tong, B.; Shi, J.; Zhi, J.; Dong, Y. Polymorphism-dependent aggregation-induced emission of pyrrolopyrrole-based derivative and its multi-stimuli response behaviors. *Dyes Pigm.* **2017**, *139*, 664−671.
(34) Sadowski, B.; Hassanein, K.; Ventura, B.; Gryko, D. T. Tetraphenylethylenepyrrolo[3,2-b]pyrrole hybrids as solid-state emitters: the role of substitution pattern. *Org. Lett.* **2018**, *20*, 3183−3186.
(35) Zhou, Y.; Zhang, M.; Ye, J.; Liu, H.; Wang, K.; Yuan, Y.; Du, Y. Q.; Zhang, C.; Zheng, C. J.; Zhang, X. H. Efficient solution-processed red organic light-emitting diode based on an electron-donating building block of pyrrolo[3,2-b]pyrrole. *ACS Appl. Mater. Interfaces* **2017**, *9*, 27875−27882.
(36) Balasubramanyam, R. K. C.; Kumar, R.; Ippolito, S. J.; Bhargava, S. K.; Periasamy, S. R.; Narayan, R.; Basak, P. Quadrupolar (A-π-D-π-A) tetra-aryl 1,4-dihydropyrrolo[3,2-b]pyrroles as single molecular resistive memory devices: substituent triggered amphoteric redox performance and electrical bistability. *J. Phys. Chem. C* **2016**, *120*, 11313−11323.
(37) Razavi, E.; Khoshsima, A.; Shahriari, R. Phase Behavior Modeling of Mixtures Containing N-, S-, and O-Heterocyclic Compounds Using PC-SAFT Equation of State. *Ind. Eng. Chem. Res.* **2019**, *58*, 11038−11059.
(38) Wang, L. Z.; Lim, T. L.; Padakanti, P. K.; Carlin, S. D.; Alavi, A.; Mach, R. H.; Prud'homme, R. K. Kinetics of Nanoparticle Radiolabeling of Metalloporphyrin with 64Cu for Positron Emission Tomography (PET) Imaging. *Ind. Eng. Chem. Res.* **2020**, *59*, 19126−19132.
(39) Chen, Y.; Jia, X.; Wang, M.; Wang, T. A synergistic effect of a ferrocenium salt on the diaryliodonium salt-induced visible-light curing of bisphenol-A epoxy resin. *RSC Adv.* **2015**, *5*, 33171−33176.
(40) Bouchikhi, N.; Bouazza, M.; Hamri, S.; Maschke, U.; Lerari, D.; Dergal, F.; Bachari, K.; Bedjaoui-Alachaher, L. Photo-curing kinetics of hydroxyethyl acrylate (HEA): synergetic effect of dye/amine photoinitiator systems. *Int. J. Ind. Chem.* **2020**, *11*, 1−9.
(41) Valdebenito, A.; Encinas, M. V. Photopolymerization of 2-hydroxyethyl methacrylate: Effect of the medium properties on the polymerization rate. *J. Polym. Sci. Polym. Chem.* **2003**, *41*, 2368−2373.
(42) Lee, T. Y.; Roper, T. M.; Jönsson, E. S.; Guymon, C. A.; Hoyle, C. E. Influence of hydrogen bonding on photopolymerization rate of hydroxyalkyl acrylates. *Macromolecules* **2004**, *37*, 3659−3665.
(43) Lu, C.-H.; Su, Y.-C.; Wang, C.-F.; Huang, C.-F.; Sheen, Y.-C.; Chang, F.-C. Thermal properties and surface energy characteristics of interpenetrating polyacrylate and polybenzoxazine networks. *Polymer* **2008**, *49*, 4852−4860.
(44) Zhou, Y.; Zhang, M.; Ye, J.; Liu, H.; Wang, K.; Yuan, Y.; Dua, Y. Q.; Zhang, C.; Zheng, C. J.; Zhang, X. H. Efficient solution-processed red organic light-emitting diode based on an electron-donating building block of pyrrolo[3,2-b]pyrrole. *Org. Electron.* **2019**, *65*, 110−115.

https://doi.org/10.1021/acsomega.1c02338
ACS Omega 2021, 6, 20902−20911

(45) Li, G. L.; Liu, J. Q.; Zhao, B. D.; Wang, T. UV spectroscopic studies and charge transfer properties of azobenzene-containing cyclopentadienyliron complexes of arenes: A combined experimental and density functional theoretical study. *Spectrochim. Acta A.* **2013**, *104*, 287−291.
(46) Ballini, R.; Petrini, M. Recent synthetic developments in the nitro to carbonyl conversion (Nef reaction). *Tetrahedron* **2004**, *60*, 1017−1047.
(47) Stewart, G.; Jiao, Y.; Valente, E. J.; Fu, P. P.; Li, T.; Hu, Z.; Yu, H. Photochemical reaction of 9-nitro-substituted anthracene-like molecules 9-methyl-10-nitroanthracene and 12-methyl-7-nitrobenz-[a]anthracene. *J. Photochem. Photobiol. A.* **2009**, *201*, 39−44.
(48) Morel, M. C.; Alers, I.; Arce, R. Photochemical degradation of 1,6-and 1,8-dinitropyrene in dolution. *Polycycl. Aromat. Comp.* **2006**, *26*, 207−219.
(49) Balasubramanyam, R. K. C.; Kandjani, A. E.; Harrison, C. J.; Rashid, S. S.; Sabri, Y. M.; Bhargava, S. K.; Narayan, R.; Basak, P.; Ippolito, S. J. 1,4-Dihydropyrrolo[3,2-b]pyrroles as a single component photoactive layer: a new paradigm for broadband detection. *ACS Appl. Mater. Interfaces* **2017**, *9*, 27875−27882.
(50) Rosa, E.; Guerrero, A.; Bosch, M. P.; Juli, L. EPR/Spin-trapping study of free radical intermediates in the photolysis of trifluoromethyl ketones with initiators. *MRC.* **2010**, *48*, 198−204.
(51) Scott, T. F.; Kowalski, B. A.; Sullivan, A. C.; Bowman, C. N.; McLeod, R. R. Two-color single-photon photoinitiation and photo-inhibition for subdiffraction photolithography. *Science* **2009**, *324*, 913−917.

https://doi.org/10.1021/acsomega.1c02338
ACS Omega 2021, 6, 20902−20911